Materials Science and Engineering C 29 (2009) 742–745

Contents lists available at ScienceDirect

Materials Science and Engineering C

journal homepage: www.elsevier.com/locate/msec

Improved dispersion of PEG-functionalized carbon nanofibers in toluene

Jian Zhao [a,b,*], Guangzhe Piao [a], Xin Wang [a], Jie Lian [c], Zhaobo Wang [a], Hongqi Hu [a], Li Chen [a], Xuyun Wang [a], Yong Tao [a], Donglu Shi [b,d]

[a] The Key Laboratory of Rubber-Plastics (Qingdao University of Science and Technology), Ministry of Education, Qingdao, 266041, China
[b] Department of Chemical and Materials Engineering, University of Cincinnati, Cincinnati, OH 45221-0012, USA
[c] Department of Mechanical, Aerospace, and Nuclear Engineering, Rensselaer Polytechnic Institute, Troy, New York 12180, USA
[d] The Institute for Advanced Materials & Nano Biomedicine, Tongji University, Shanghai, China

ARTICLE INFO

Article history:
Received 30 September 2008
Received in revised form 15 December 2008
Accepted 18 February 2009
Available online 5 March 2009

Keywords:
Carbon nanofibers
Dispersion
Light scattering
Functionalization

ABSTRACT

Small-angle light scattering is used to assess the dispersion of poly(ethylene glycol) (PEG)-functionalized carbon nanofibers suspended in toluene. Analysis of these data show PEG-functionalized and untreated nanofibers exhibit hierarchical morphology consisting of small-scale aggregates (small bundles) that agglomerate to form fractal clusters. The bundles consist of multiple tubes possibly aggregated side-by-side. Functionalization has little effect on this bundle morphology. Rather, functionalization inhibits agglomeration of the bundles. For untreated fibers, large agglomerates appear immediately after cessation of sonication, whereas for functionlized nanofibers, the size of agglomerates is substantially reduced and they do not grow over time due to the presence of PEG oligomers on the surfaces of the nanofibers. Functionalization leads to improved dispersion by inhibiting agglomeration, not by disrupting the side-by-side bundles.

1. Introduction

The carbon nanotubes, discovered by Iijima [1], have unusual mechanical properties and intriguing electronic properties, leading to a wide range of potential uses [2,3]. Unfortunately, the advantages of carbon nanotubes have not been realized because of the difficulty of obtaining fully dispersed nanotubes [4]. To date, the most successful approaches to dispersion of carbon nanotubes involve functionalization of the sidewalls and tube tips [5–8]. Although many groups have achieved functionalization of carbon nanotubes, measurement of the degree of dispersion remains challenging.

Poly(ethylene glycol), PEG, has been the most widely studied and accepted biomaterial. For example, co-adsorption of Triton and PEG is very effective for preventing nonspecific adsorption of streptavidin on nanotubes [9]. Attachment of PEG on carbon nanotubes is not only useful for biomedical applications, but also leads to improved dispersion. Here we use light scattering to quantify dispersion of PEG-functionlized carbon nanofibers and make a comparison with untreated nanofibers.

The presence of oxygen-containing groups on carbon nanotubes after acid treatment provides rich chemistry for the attachment of moieties to the surface of nanotubes. The simplest route to functionalization of the carbon nanotubes is to directly react an amine with the carboxylated nanotubes. A zwitterion is produced through a simple acid–base reaction. This method produces nanotubes that are soluble in water or organic solvents, depending on the chosen functional molecules. Research demonstrates that full-length nanotubes can be solubilized (>0.5 mg/mL) in tetrahydrofuran and 1,2-dichlorobenzene by the functionalization of sidewall defects after treatment by HNO3 [7]. Sun et al reported that polymer-bound carbon nanotubes could be formed by attaching nanotubes to linear polymers such as poly(ethylene glycol) (PEG) via acid–base zwitterionic interaction [10]. It proved that PEG-functionalized nanofibers are well dispersed in water. Here we show that PEG-functionalized nanofibers are also well dispersed in organic solvents such as toluene.

Dispersions of functionalized carbon nanotubes have been characterized by atomic force microscopy (AFM), UV/visible and Raman spectra etc [11,12]. We [13–22] have recently used scattering methods to determine the morphology of carbon nanotube suspensions and composites. Here, we use scattering to quantify the dispersion of PEG-functionalized carbon nanofibers suspended in toluene and make comparisons with untreated nanofibers.

Light scattering data are analyzed to show that the PEG-functionalized fibers show improved dispersion and do not agglomerate over time. They do not exist as individually suspended tubes, but as side-by-side aggregates or bundles. Untreated treated fibers also exist as bundles, but in this case the bundles agglomerate immediately and precipitate rapidly.

2. Experimental section

Multi-walled nanofibers (product number PR19-LHT) were provided by Pyrograf Products Inc. (www.apsci.com). Pyrograf®-III PR19-HT nanofibers are vapor-grown and subsequently heated to temperatures up to 3000 °C. The multi-walled nanofibers (MWNFs) normally

* Corresponding author.
E-mail address: zhaojian@gmail.com (J. Zhao).

0928-4931/$ – see front matter © 2009 Elsevier B.V. All rights reserved.
doi:10.1016/j.msec.2009.02.014

contain a few concentric cylinders but may also be nested truncated cones. Typically the cores are open.

The carbon nanofibers were treated to attach carboxylic acid groups to their surfaces. The acid treatment procedure was as follows: A 100 mg of nanofibers was added to 400 ml of a mixture 98% H_2SO_4–70% HNO_3 (3:1). The mixture was subject to ultrasonication for 4 h. The resulting mixture was diluted with deionized water to 2000 ml, and then filtered through a PTFE membrane disc filter (Gelman, 0.2 μm pore size) followed by washing several times with deionized water until no residual acid was present. The sample was dried in a vacuum oven.

PEG-functionalized nanofibers were prepared as follows: a dried acid-treated nanofiber sample (50 mg) was mixed with diamine-terminated oligomeric poly(ethylene glycol), O,O′-bis(3-aminopropyl) poly(ethylene glycol)1500 (PEG_{1500N}) (Aldrich, 500 mg), and the mixture was vigorously stirred at 100 °C for 5 days under nitrogen protection. Deionized water was added to the mixture, and the resulting dispersion was placed in membrane tubing (cutoff molecular weight ~12,000) for dialysis against deionized water for 3 days. The water was changed every 8 h. A homogenous dark-colored solution of PEG-functionalized nanofibers was obtained after the solid residue was separated from the dispersion by centrifuging. The sample was collected by PTFE membrane filtration (0.45 μm pore size), followed by washing with ethanol and drying at room temperature under vacuum.

TEM samples were prepared by allowing a drop of nanofiber suspensions to dry onto carbon film. The high-resolution transmission electron microscopy (HRTEM) experiments were performed using a JEOL JEM 2010F electron microscope with a field emission source. The accelerating voltage used was 200 kV.

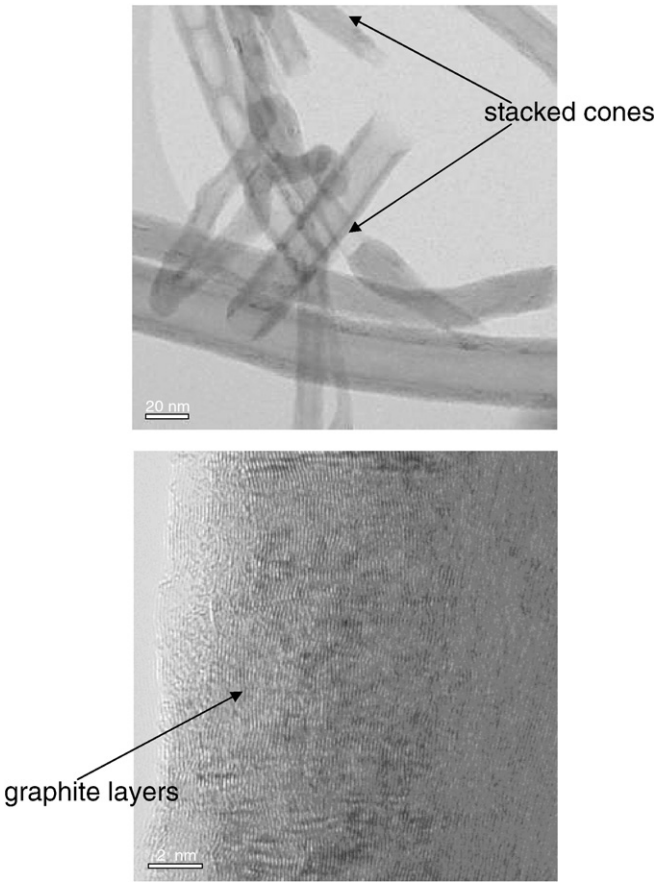

Fig. 1. TEMs of unmodified carbon nanofibers at two magnifications. Graphitic layers are visible at both magnifications. The low-resolution image (top) shows a variety of tube shapes and morphologies including concentric cylinders and stacked cones. No metallic catalyst particles are observed. The bars are 20 nm and 2 nm.

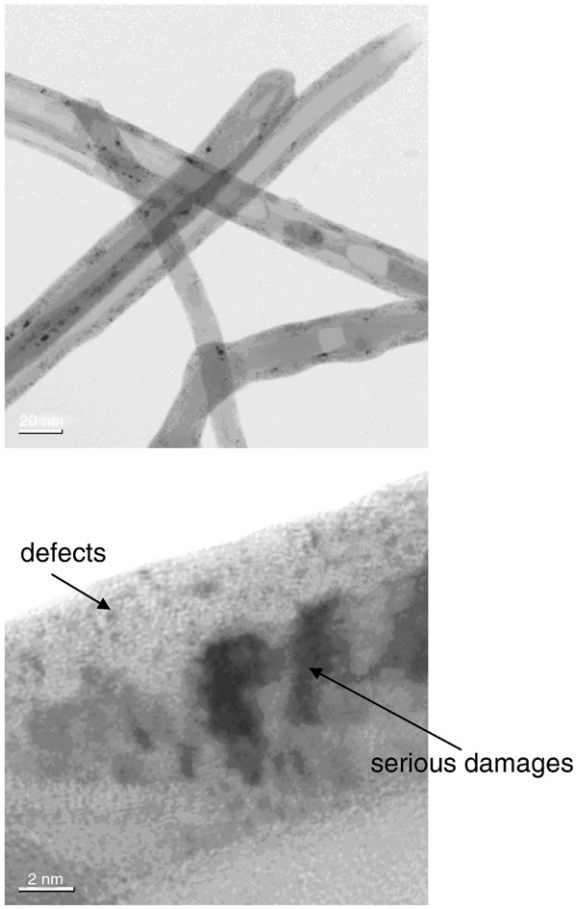

Fig. 2. TEMs of acid-treated and subsequently PEG-functionalized carbon nanofibers at two magnifications. Defects and serious damage on the walls are evident as well as breakage of graphite layers. The bars are 20 nm and 2 nm.

The dispersion efficiency was determined using a low-angle light scattering photometer—a Micromeritics Saturn Digisizer 5200 (www.micromeritics.com). Light scattering covers the regime 10^{-6} Å^{-1}<q<10^{-3} Å^{-1}, where q is the magnitude of the scattering vector, $q=(4\pi \sin\theta)/\lambda$, where θ is half the scattering angle, and λ is the wavelength of the radiation in the medium. The q-range corresponds to length-scales ($\sim q^{-1}$) from 100 μm at low q to 1000 Å (0.1 μm) at high q.

3. Results and discussion

The raw Pyrograf®-III PR19HT powder consists of loosely aggregated nanofibers. Fig. 1 shows a HRTEM image of the powder. Defects on the sidewalls of nanofibers are occasionally observed. The graphite structure with the interlayer spacing $d=0.34$ nm is clearly observed. No iron catalyst particles are found by TEM.

The bright field and high-resolution TEM images of the acid-treated carbon nanofibers are shown in Fig. 2. Many defects formed on the sidewall and serious damage appears after oxidation. Disruption of outer graphitic layers is observed in the TEM image. The stripping of the altered outer graphite layers after strong oxidation can thin nanofibers. These observations are in agreement with literature [11,23]. PEG-functionalized nanofibers look similar to acid-treated nanofibers in high resolution TEM.

There is considerable experimental evidence for the presence of carboxylic acid groups bound to carbon nanotubes after acid treatment [6,24]. Exploiting acid–base zwitterionic interactions, diamine-terminated oligomeric PEG was reacted with the carboxylic acids anchored on the surface of carbon nanofibers. PEG is a soluble

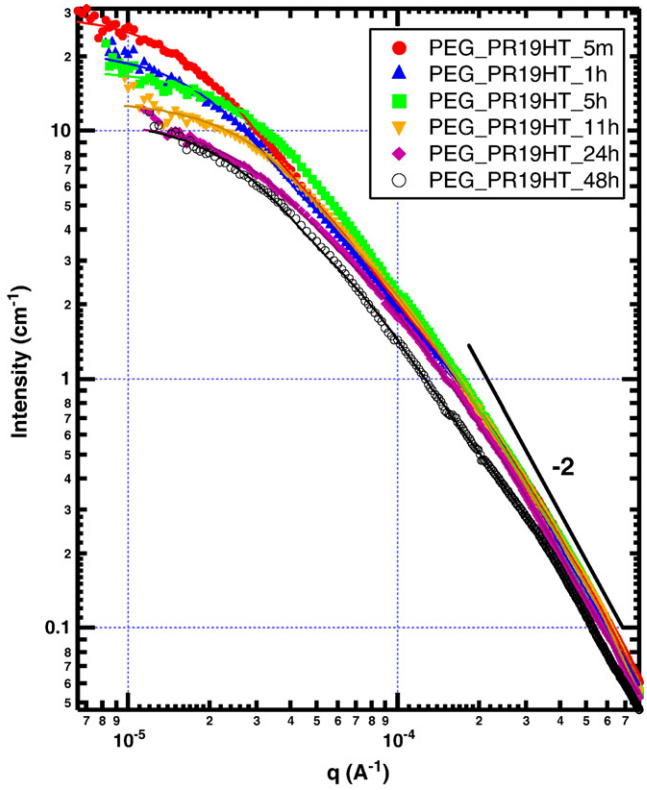

Fig. 3. Evolution of the light scattering profile of PEG-functionalized nanofibers for 2 days. The suspensions were sonicated at 10 W for 5 min before the observations began. The measurements were taken in the batch mode, so the sample was undisturbed during the course of the observations. The lines are two-level unified fits. The unified parameters are collected in Table 1.

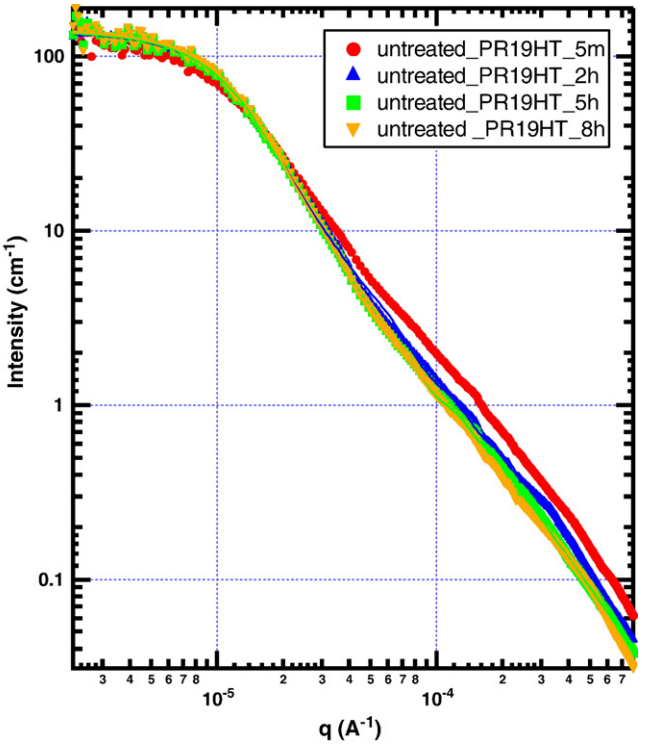

Fig. 4. Evolution of the light scattering profile of untreated nanofibers for 8 h. The suspensions were sonicated at 10 W for 5 min before the observations began. The measurements were taken in the batch mode, so the sample was undisturbed during the course of the observations. Note that the intensity at small q is nearly a factor of 10 larger than Fig. 3, implying larger aggregated structures. The lines are two-level unified fits. The unified parameters are collected in Table 2.

polymer in toluene. The resulting PEG-functionalized sample forms a dark-colored homogeneous solution that is stable in toluene for weeks. This dispersion was characterized using light scattering.

Fig. 3 shows the light scattering profiles as a function of time for PEG-functionalized carbon nanofibers in toluene at a concentration of 5.0×10^{-6} g/ml. The data were obtained in the batch mode with no circulation or sonication. That is, the sample chamber was filled with the undiluted suspension and observed without stirring, agitation or circulation. Toluene was used as background.

The scattered intensity decreases with time at low-q. After 48 h, the intensity does not show any increase, implying no agglomeration. Two "knees" are observed indicating two length scales. The knee region is referred to as Guinier scattering. The curvature in the Guinier regime defines a length scale (Guinier radius or radius-of-gyration, R_g, in the case of independent scatterers). Each Guinier knee is followed by a quasi power-law regime. The curves were fit using Beaucage's Unified Model to extract R_g, the power-law exponents, P, and the Guinier prefactors, G, and power-law prefactor, B, associated with each length scale [25]. These parameters are displayed in Table 1 for the two structural levels.

The slope near -2 ($P=2$) on a log–log plot around $q=0.002$ Å^{-1} could arise from a hollow tube since the wall of such an object is a two-dimensional on scales larger than its wall thickness and shorter than the radius. Such a slope, however, can also arise from more complex aggregated structures [13,14]. The crossover length scale ($q^{-1}\cong1$ μm) between the two power-law regimes corresponds to the largest radius of the tube aggregates. Minimal change in R_g and P is observed for $q>10^{-4}$ Å^{-1}, indicating minimal change in morphology with time on length scales below ~1 μm.

As shown in Fig. 3, the R_g extracted from high-q region is considerably larger than the tube diameters seen in TEM. That is, the scattering entities are not individual fibers, but bundles thereof. Fibers likely form side-by-side aggregates that are never disrupted. It doesn't take much aggregation to produce such aggregates.

We also monitored dispersion behavior of untreated carbon nanofibers although such a suspension is quite unstable in toluene even. Tubes precipitate rapidly. The data for the untreated sample (Fig. 4) show similarities and differences when compared to the PEG-functionalized samples. Two structural levels are present and the

Table 1
Guinier radii and exponents as a function of time for PEG-functionalized carbon nanofibers.

	Time	5 min	1 h	5 h	11 h	24 h	48 h
Low q	R_g (μm)	7.5	6.7	4.5	4.3	4.4	5.0
	P	1.70	1.84	1.82	1.85	1.87	1.65
	G	28.93	20.56	17.52	13.03	10.61	10.52
	10^8 B	22.50	57.2	10.21	7.00	8.81	3.22
High q	R_g (μm)	0.78	0.76	0.76	0.72	0.62	0.55
	P	1.87	1.85	1.87	1.96	1.89	1.81
	G	0.68	0.81	0.41	0.47	0.38	0.28
	10^7 B	2.0	2.39	0.76	0.16	0.76	7.51

Table 2
Guinier radii and exponents as a function of time for untreated carbon nanofibers.

	Time	5 min	2 h	5 h	8 h
Low q	R_g (μm)	14.4	13.5	13.6	13.4
	P	2.06	2.19	2.01	2.30
	G	156.84	138.38	139.39	142.1
	10^9 B	6.36	0.46	0.16	0.24
High q	R_g (μm)	0.82	0.91	0.85	0.96
	P	2.00	2.02	2.04	2.07
	G	0.68	1.06	0.72	0.70
	10^8 B	2.74	2.27	1.74	0.61

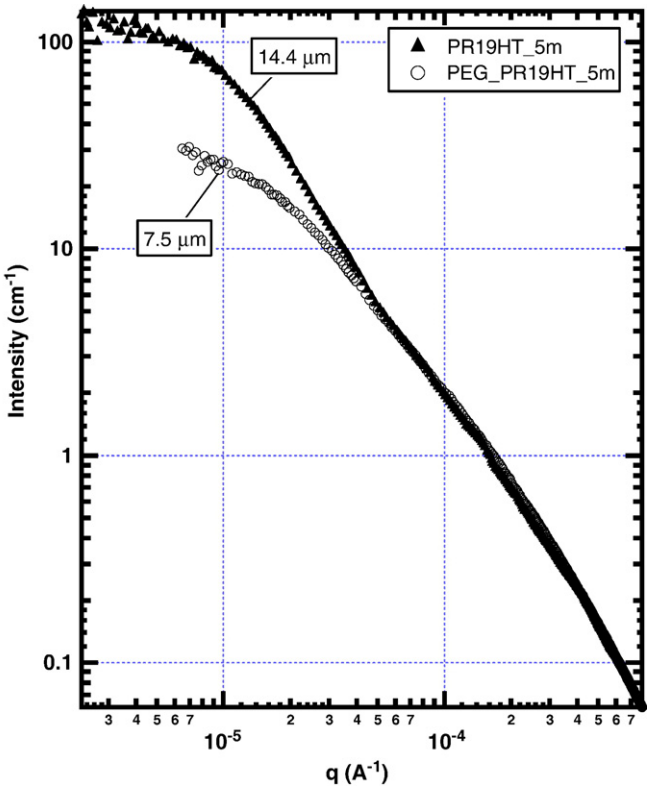

Fig. 5. Comparison of the scattering profiles for PEG-functionalized and untreated carbon nanofibers at 5 min. The suspensions were sonicated at 10 W for 5 min before data were taken using light scattering in batch mode. A substantial population large-scale clusters is present for the untreated sample.

high-q features are similar to the functionalized nanofibers. The overall intensity is almost unchanged with time. For the as-received sample, however, the large-scale agglomerates are observed immediately (5 min)., The R_gs extracted from low-q region correspond to the size of agglomerates and are substantially larger than PEG-functionalized samples as shown in Table 2. Functionalization does not change the gross morphology of the nanotube aggregates, but only inhibits agglomeration of these smaller scale aggregates.

Fig. 5 compares the scattering profile for PEG-functionalized and as-received carbon nanofibers at 5 min after sonication. The intensity at low q (prefactor, G) for the PEG-functionalized sample is nearly one order of magnitude smaller than that for the untreated one, indicating smaller entities in former suspension. Detailed analysis shows that the low-q Guinier radius is 7.5 μm for PEG-functionalized nanofibers, compared to 14.4 μm for untreated nanofibers. These observations are consistent with improved dispersion due to the presence of PEG oligomers on the surface.

Compared to the untreated samples, PEG-functionalized nanofibers do not show agglomeration with time. The homogeneous solution is stable in toluene for weeks. Attachment of PEG oligomers to nanofibers alters the surface properties of nanofibers and renders the fibers more compatible with toluene, thus controlling agglomeration.

4. Conclusion

We have compared dispersion behavior of PEG-functionalized and untreated nanofibers suspended in toluene under quiescent conditions. Both samples show a hierarchical morphology consisting small-scale aggregates and large-scale agglomerates. The aggregates are not individual tubes, but side-by-side bundles (aggregates) of tubes. In any case these objects agglomerate to form large-scale fractal clusters. Functionalization has minimal effect on the small-scale bundle morphology. Compared to untreated nanofibers which form large agglomerates immediately, the PEG-functionalized sample do not agglomerate over time and remain stable for weeks. The presence of the PEG oligomers leads to improved dispersion of nanofibers by suppressing agglomeration, not by disrupting side-by-side aggregates.

Acknowledgments

We thank Dale W. Schaefer at University of Cincinnati for his guideline in light scattering. The University of Dayton Research Institute supported work at the University of Cincinnati. The work was funded in part by Doctoral Fund of Qingdao University of Science and Technology and the Key Laboratory of Rubber–Plastics (Qingdao University of Science and Technology), Ministry of Education, China.

References

[1] S. Iijima, Nature 354 (1991) 56.
[2] L.M. Dai, A.W.H. Mau, Adv. Mater. 13 (2001) 899.
[3] P.G. Collins, A. Zettl, H. Bando, A. Thess, R.E. Smalley, Science 278 (1997) 100.
[4] J. Chen, M.A. Hamon, H. Hu, Y.S. Chen, A.M. Rao, P.C. Eklund, R.C. Haddon, Science 282 (1998) 95.
[5] P.J. Boul, J. Liu, E.T. Mickelson, C.B. Huffman, L.M. Ericson, I.W. Chiang, K.A. Smith, D.T. Colbert, R.H. Hauge, J.L. Margrave, R.E. Smalley, Chem. Phys. Lett. 310 (1999) 367.
[6] J. Liu, A.G. Rinzler, H.J. Dai, J.H. Hafner, R.K. Bradley, P.J. Boul, A. Lu, T. Iverson, K. Shelimov, C.B. Huffman, F. Rodriguez-Macias, Y.S. Shon, T.R. Lee, D.T. Colbert, R.E. Smalley, Science 280 (1998) 1253.
[7] J. Chen, A.M. Rao, S. Lyuksyutov, M.E. Itkis, M.A. Hamon, H. Hu, R.W. Cohn, P.C. Eklund, D.T. Colbert, R.E. Smalley, R.C. Haddon, J. Phys. Chem. B 105 (2001) 2525.
[8] E.T. Mickelson, I.W. Chiang, J.L. Zimmerman, P.J. Boul, J. Lozano, J. Liu, R.E. Smalley, R.H. Hauge, J.L. Margrave, J. Phys. Chem. B 103 (1999) 4318.
[9] M. Shim, N.W.S. Kam, R.J. Chen, Y. Li, H. Dai, Nano lett. 2 (2002) 285.
[10] W.J. Huang, S. Fernando, L.F. Allard, Y.P. Sun, Nano lett. 3 (2003) 565.
[11] M.S.P. Shaffer, X. Fan, A.H. Windle, Carbon 36 (1998) 1603.
[12] K.D. Ausman, R. Piner, O. Lourie, R.S. Ruoff, M. Korobov, J. Phys. Chem. B 104 (2000) 8911.
[13] D.W. Schaefer, J.M. Brown, D.P. Anderson, J. Zhao, K. Chokalingam, D. Tomlin, J. Ilavsky, J. Appl. Crystallogr. 36 (2003) 553.
[14] D.W. Schaefer, J. Zhao, J.M. Brown, D.P. Anderson, D.W. Tomlin, Chem. Phys. Lett. 375 (2003) 369.
[15] J.M. Brown, D.P. Anderson, R.S. Justice, K. Lafdi, M. Belfor, K.L. Strong, D.W. Schaefer, Polymer 46 (2005) 10854.
[16] D.W. Schaefer, R.S. Justice, Macromolecules (2007) 40 8501.
[17] C. Zhao, G. Hu, R. Justice, D.W. Schaefer, S. Zhang, M. Yang, C.C. Han, Polymer 46 (2005) 5125.
[18] B.J. Bauer, J.A. Fagan, E.K. Hobbie, J. Chun, V. Bajpai, J. Phys. Chem., C 112 (2008) 1842.
[19] B.J. Bauer, E.K. Hobbie, M.L. Becker, Macromolecules 39 (2006) 2637.
[20] J.A. Fagan, B.J. Landi, I. Mandelbaum, J.R. Simpson, V. Bajpai, B.J. Bauer, K. Migler, A.R. Hight Walker, R. Raffaelle, E.K. Hobbie, J. Phys. Chem., B 110 (2006) 23801.
[21] H. Wang, W. Zhou, D.L. Ho, K.L. Winey, J.E. Fischer, C.J. Glinka, E.K. Hobbie, Nano lett. 4 (2004) 1789.
[22] W. Zhou, M.F. Islam, H. Wang, D. Ho, A.G. Yodh, K.I. Winey, J.E. Fischer, Chem. Phys. Lett. 384 (2004) 185.
[23] M. Monthioux, B.W. Smith, B. Burteaux, A. Claye, J.E. Fischer, D.E. Luzzi, Carbon 39 (2001) 1251.
[24] H. Hu, P. Bhowmik, B. Zhao, M.A. Hamon, M.E. Itkis, R.C. Haddon, Chem. Phys. Lett. 345 (2001) 25.
[25] G. Beaucage, D.W. Schaefer, J. Non-Cryst. Solids 172–174 (1994) 797 805 172 174 (1994) 797 805.